Available online at www.sciencedirect.com
ScienceDirect
Journal of Hazardous Materials 147 (2007) 370–380
Journal of Hazardous Materials
www.elsevier.com/locate/jhazmat

Cationic polyelectrolyte/bentonite prepared by ultrasonic technique and its use as adsorbent for Reactive Blue K-GL dye

Qian Li [a], Qin-Yan Yue [a,*], Yuan Su [b], Bao-Yu Gao [a], Lin Fu [a]

[a] School of Environmental Science and Engineering, Shandong University, Jinan 250100, Shandong, PR China
[b] Department of Mathematics and Statistics, Shandong Economic University, Jinan 250014, Shandong, PR China

Received 30 September 2006; received in revised form 3 January 2007; accepted 4 January 2007
Available online 12 January 2007

Abstract

In this study, the cationic polyelectrolyte polyepicholorohydrin-dimethylamine (EPI-DMA) was intercalated into bentonite using ultrasonic. The structure of EPI-DMA/bentonite and its adsorption of Reactive Blue K-GL (RB K-GL) dye were investigated. Compared with raw bentonite, the EPI-DMA/bentonite had larger interlayer spacing and was more hydrophobic, providing with better surface properties for adsorption. The adsorption of RB K-GL on EPI-DMA/bentonite was described by the adsorption models of Langmuir, Freundlich and Dubinin–Radushkevic. The adsorption kinetics was analyzed using pseudo-first- and second-order kinetic models and intraparticle diffusion model. Results showed that both the intraparticle diffusion and first-order adsorption occur in the initial period of adsorption, and that pseudo-second-order kinetic model was more suitable for describing the whole adsorption process. The reaction rates were also calculated. The changes of free energy, enthalpy and entropy of adsorption were evaluated for the adsorption of RB K-GL onto EPI-DMA/bentonite, suggesting that the adsorption process was spontaneous and exothermic.

Keywords: Cationic polyelectrolyte/bentonite; Reactive dye; Adsorption; Kinetics; Thermodynamics

1. Introduction

Various types of dyes appear in wastewater effluents from textiles, printing, and dyestuffs, as well as the food and paper-making industries. Water-soluble anionic dyes—reactive dyes are the most commonly dyes used for application ease, bright colors, and excellent colorfastness [1,2]. It is estimated that 10–20% of reactive dye remains in wastewater during production and nearly 50% of reactive dyes may be lost to the effluents during dyeing process [3,4], due to its high water-solubility. Reactive dyes are typically azo-based chromophores combined with different types of reactive groups, primarily based on substituted aromatic and heterocyclic groups [5]. Many reactive dyes are toxic to some organisms and hence harmful to aquatic animals [6]. Furthermore, some dyes and their reaction products, such as aromatic amines, possess high carcinogenicity [4].

The removal of dyes before the disposal of wastewater is necessary. Due to poor biodegredation of dyes, especially those containing azo-groups, under aerobic conditions [7], a conventional biological wastewater treatment process is not suitable [4]. Therefore, investigations have been conducted for different approaches such as adsorption, oxidation–ozonation, coagulation–flocculation, membrane processes, etc. [5,8]. Adsorption is one of the most efficient processes to remove dyes from wastewater, which provides an alternative treatment, especially if the adsorbent is cheap and widely available [9]. Activated carbon is the most widely used adsorbent for industrial applications, but it is expensive for each adsorption cycle [10,11]. Therefore, it is important to find less expensive, more efficient, and locally available materials for the removal of color from wastewaters.

Clays [12,13] especially chemically modified clays [11,14–16] have been identified as an innovative and promising class of adsorbent materials for this purpose. Bentonite is a clay mineral, which is mainly composed of montmorillonite. It is a 2:1 type aluminosilicate, which unit layer structure consists of one $A1^{3+}$ octahedral sheet placed between two Si^{4+}tetrahedral

* Corresponding author. Tel.: +86 531 88365258; fax: +86 531 88364513.
E-mail addresses: liqian@mail.sdu.edu.cn (Q. Li), qyyue58@yahoo.com.cn (Q.-Y. Yue), ysu1979@163.com (Y. Su), bygao@sdu.edu.cn (B.-Y. Gao), treehua@163.com (L. Fu).

0304-3894/$ – see front matter © 2007 Elsevier B.V. All rights reserved.
doi:10.1016/j.jhazmat.2007.01.024

sheets. Replacing the exchangeable inorganic cations (e.g. Na^+, Ca^{2+}, H^+) on the internal and external surfaces of montmorillonite with organic cations, enhances the adsorption capacity as the bentonite surfaces change from hydrophilic to hydrophobic [17]. Therefore, organophilic bentonite has been used extensively for a wide variety of environmental applications [18].

In addition, both the advances in the preparation method and the increase of the kinds of organic cations promote the development of organobentonite as adsorbents for environmental and economical purposes [19,20]. Recently, sonochemical cavitation exerted by ultrasound has become a method of concentrating the diffuse energy of sound to prepare novel materials [21]. As a result, the intercalation of compounds into layered inorganic solids using ultrasonic has attracted the researchers' attention greatly [21,22]. Moreover, cationic polyelectrolytes, which are suitable for rendering clays more hydrophobic to remove hydrocarbon from water, also broaden the range of organobentonite [19,23]. Previous studies showed that cationic polyelectrolyte/bentonite complexes could not only make bentonite more hydrophobic but also develop a net positive charge [23–25], which would be suitable to remove negatively charged pollutants from wastewater. Polyepicholorohydrin-dimethylamine (EPI-DMA), which is a new effectively water-soluble cationic polyelectrolyte with amidocyanogen and ammonium ion [26], has the potential to fulfill the main requirements for preparing organophilic bentonite. Our previous study also indicated that cationic polyelectrolyte/bentonite prepared by EPI-DMA is a good adsorbent for disperse dyes [27,28].

Many previous studies have been carried out to investigate the adsorption of anionic dyes onto organobentonite. However, the adsorption of an anionic reactive dye, such as Reactive Blue K-GL (RB K-GL), onto cationic polyelectrolyte/bentonite has not been examined. Thus, in present work, a new adsorbent, EPI-DMA cationic polyelectrolyte/bentonite (EPI-DMA/bentonite), was prepared using ultrasonic technique. Also investigated in this study is the possibility of the adsorbent for removal of RB K-GL dye from aqueous solution by adsorption method. Batch isotherm and kinetic experiments were performed and modeled by different isotherm equations and kinetic equations. The calculated thermodynamic parameters from the isotherm constant were used to explain the nature of adsorption.

2. Materials and methods

2.1. Materials

The dye used in this study is Reactive Blue K-GL (RB K-GL) (Color Index number 18245), obtained from Bin Zhou Dye Printing Co. (Shandong, China). The chemical structure of RB K-GL is depicted in Fig. 1a, where "CuPc" is the abbreviation of "copper phthalocyanine" and its structure is shown in Fig. 1b. Absorbance values were recorded at the corresponding maximum absorbance wavelength 597 nm.

The Na^+-exchanged form of bentonite used in this study was obtained from the city of Weifang in Shandong, China. It contains about 95% montmorillonite with the chemical composition of 69.32% SiO_2, 14.27% Al_2O_3, 1.99% CaO, 2.69% MgO, 1.84% Fe_2O_3, 1.85% Na_2O, 1.38% K_2O as reported by the supplier. The cation exchange capacity (CEC) of the clay, measured by the methylene blue method [29], was 700 mmol/kg.

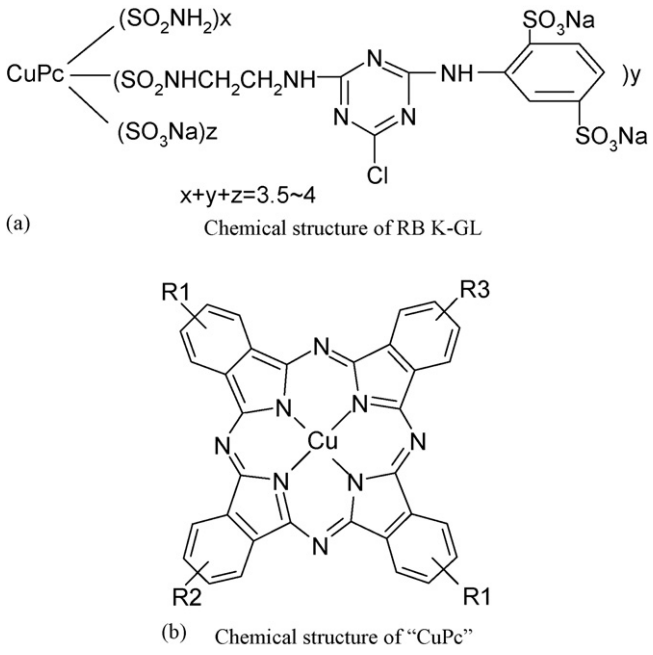

Fig. 1. Chemical structure of Reactive Blue K-GL (RB K-GL).

The cationic polyelectrolyte polyepicholorohydrin-dimethylamine (EPI-DMA) was produced by Bin Zhou Chemical Co. (Shandong, China), which has a viscosity of 400 mPa/s, and a cationic degree of 3.6 mmol/g. The formula is

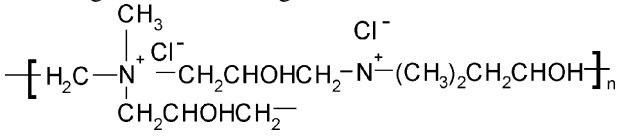

where the value of n is in the range of 400–600.

2.2. Preparation of EPI-DMA/bentonite

To prepare the cationic polyelectrolyte/bentonite, about 20 g of oven-dried clay was directly added to 100 ml solution containing the respective EPI-DMA equal to twice of the cation exchange capacity of the bentonite. Then, the whole mass was ultrasonicated at room temperature for 30 min with the help of an ultrasonic bath (KQ3200E, China, 40 kHz). The complex was separated from the mixture by vacuum filtering and washing several times with deionized water. The cationic polyelectrolyte/bentonite complex was dried at 60 °C in an oven and activated for 1 h at 105 °C, and then stored for further use. This modified bentonite is designated as EPI-DMA/bentonite.

Furthermore, in order to eliminate the effect of water on the basal spacing of bentonite, we prepared water-washed bentonite at the same condition with that of the EPI-DMA/bentonite preparation. The experiment condition was as follows.

About 20 g of oven-dried clay was directly added to 100 ml deionized water. Then, the whole mass was ultrasonicated at

room temperature for 30 min with the help of an ultrasonic bath. The bentonite was separated from the mixture by vacuum filtering, dried at 60 °C in an oven and activated for 1 h at 105 °C. This bentonite is designated as water-washed bentonite.

The clay samples were analyzed by X-ray powder diffraction using a D/max-RB diffractometer with Cu Kα radiation. TGA thermograms of Na-bentonite and EPI-DMA/bentonite were recorded at a heating rate of 10 °C/min up to 800 °C under N_2 condition using a SDT Q600 (TA Co., USA) thermogravimetric analyzer in the range 10–800 °C.

2.3. Adsorption experiments

The adsorption experiments were carried out by using a sample having 0.1 g of EPI-DMA/bentonite and 100 ml of dye solution in 250 ml flasks and shaking on a horizontal shaker. The pH experiments were conducted with 50 mg/l of dye solutions at 296 K for 2 h. The pH was carefully adjusted between 1 and 13, adding a small amount of dilute HCl or NaOH solution using a pH meter. In the highly pHs (pH > 9) experiments, the accumulated and sedimentated dye was filtrated before the adsorption. The solutions initial pH value was used throughout all adsorption experiments, which were performed at various initial concentrations (0–100 mg/l), time intervals and temperatures (23, 28 and 33 °C) to determine the adsorption equilibrium time and the maximum adsorption amount of dye. The solution was filtered and then analyzed quantitatively. The dye concentration in the clear supernatant was then determined by spectrophotometric method. All measurements were recorded at the wavelength corresponding to maximum absorbance, λ_{max}, which is 597 nm for RB K-GL, using spectrophotometer (UV-754). The reproducibility during concentration measurements was ensured by repeating the experiments three times under identical conditions and calculating the average values. Standard deviations of experiments were found to be within ±5.0%. The amount of adsorbed dye, Q (mg/g), under different conditions was calculated by

$$Q = \frac{V(C_0 - C_e)}{W} \quad (1)$$

where C_0 and C_e are the initial and equilibrium concentrations (mg/l), respectively, V the volume of dye solution (ml) and W is the weight (g) of EPI-DMA/bentonite adsorbent.

The study of adsorption isotherms was performed using dye solution at various concentrations for 2 h to allow attainment of equilibrium at constant temperatures of 23, 28 and 33 °C. The initial concentration of 50 mg/l dye solution was selected for the kinetics study at different temperatures (23, 28 and 33 °C), and the adsorption amount was determined at different time intervals.

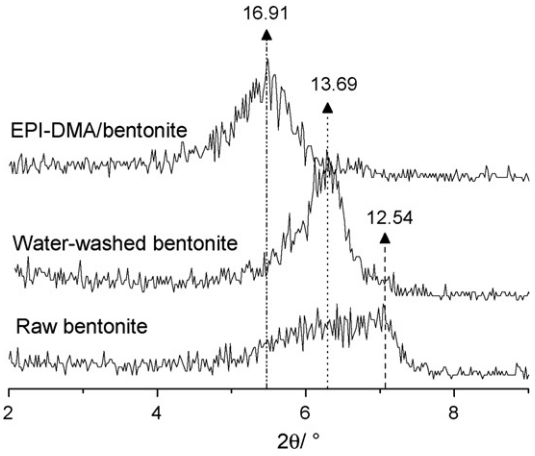

Fig. 2. XRD patterns of raw bentonite, water-washed bentonite and EPI-DMA/bentonite.

3. Results and discussion

3.1. XRD analysis of EPI-DMA/bentonite

X-ray diffraction analysis was performed to investigate the effects of intercalary molecular on the basal spacing of bentonite. The variation in the basal spacing of bentonite structure resulting from intercalation process is a strong indicator of the extent of intercalary molecular reaching the interlamellar sorption sites [30]. The exchangeable inorganic cations (e.g. Na^+, Ca^{2+}, H^+) on the internal and external surfaces of bentonite could be replaced by the amidocyanogen of EPI-DMA to form EPI-DMA/bentonite and the process can be explained as follows:

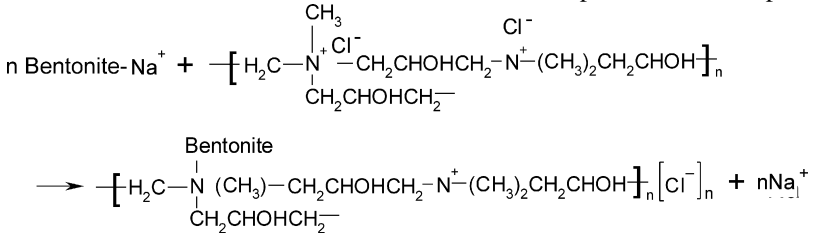

The characterisation and the intercalation process were also reported by Breen [31]. In the case of our study, we also had reported the formation and characteristics of EPI-DMA/bentonite complexes [32].

In this study, all the samples used for XRD analysis were dried at 105 °C, which ensured the desorption of physically adsorbed water of the surface layer. Then basal spacing of each sample was calculated using Bragg's law:

$$2d \sin\theta = m\lambda \quad (2)$$

where d is the basal spacing (Å), θ the angle of diffraction (°), λ the wavelength (nm), and m is the path differences between the reflected waves which equals an integral number of wavelengths (λ). The XRD patterns of the raw bentonite, water-washed bentonite and EPI-DMA/bentonite sample are shown in Fig. 2.

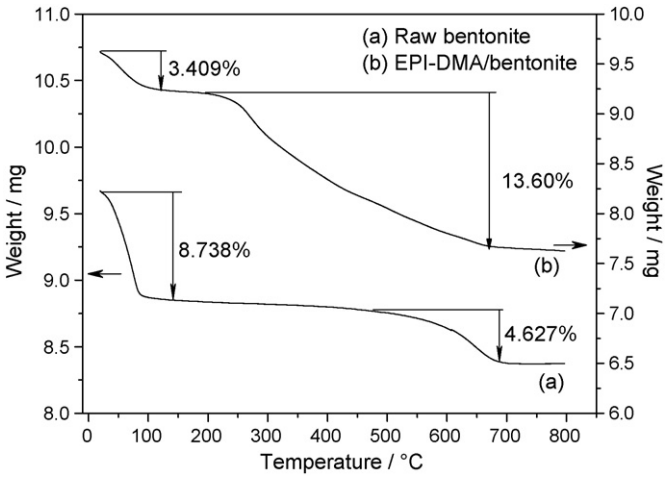

Fig. 3. TGA thermograms of raw benonite (a) and EPI-DMA/benonite (b).

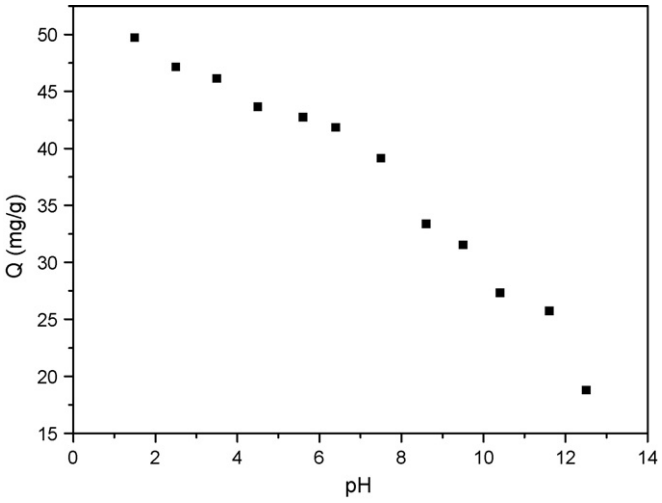

Fig. 4. Effect of pH on adsorption of RB K-GL onto EPI-DMA/bentonite.

The 2θ peaks for air-dried raw, water washed and EPI-DMA/bentonite were 7.23°, 6.28° and 5.36°. The calculated basal spacing of the samples according to the 2θ peaks were 12.54, 13.69 and 16.91 Å, respectively. This observation suggested that EPI-DMA molecules intercalated into the interlayers of bentonite and the interlayer space was extended.

3.2. TGA analysis

In order to obtain further evidence for the intercalation of EPI-DMA cationic polyelectrolyte into the silicate lattice, TGA diagrams were recorded. The TGA plots of raw and EPI-DMA/bentonite are shown in Fig. 3. For raw bentonite, the TGA diagram exhibited mass losses of 8.738% below 100 °C, which could be attributed to the desorption of physically adsorbed water of the surface layer; 4.627% losses in the range of 500–700 °C, which could be attributed to the dehydroxylation of the aluminosilicate layer. The mass losses of EPI-DMA/bentonite sample were 3.409% below 243 °C for the desorption of physically adsorbed water and 13.60% at 243–670 °C for both the decomposition of polyelectrolyte intercalated in the layers and the dehydroxylation of the clay layers.

3.3. Effect of solution pH

The pH value of the solution, which affects the surface charge of the adsorbent and the degree of speciation of adsorbate [11], was an important controlling parameter in the adsorption process. The adsorption of RB K-GL onto EPI-DMA/bentonite was carried out to examine the effect of pH (in a range of 1–13). As can be seen in Fig. 4, the adsorption capacity of RB K-GL onto EPI-DMA/bentonite decreases significantly with increase the of pH. The RB K-GL dye is reactive dyestuff. There are $-SO_3^-$ groups in its structure. In the dye-EPI-DMA/bentonite adsorption system, at strongly acidic pHs, the protonation of $-SO_3^-$ groups increases and more $-SO_3Na$ of dye molecule exists as $-SO_3H$, which can react with the amidocyanogens of EPI-DMA to form $-NH^{2+}\ SO_3^-$ or $=NH^+\ SO_3^-$ [33]. In addition, according to the theory of Lewis acidic and basic, at low pH values, the dye bears strong negative charge due to the increases of the protonation of $-SO_3^-$ groups [5,34,35], thereby a significantly high electrostatic attraction existing between the positively charged adsorption sites and the negatively charged dyes [36]. As a result, the adsorption of reactive dye anions onto EPI-DMA/bentonite is significantly enhanced. But as the pH of the system increases, the protonation of $-SO_3^-$ groups decreases and consequently the negative charge of reactive dye decreases. In strongly alkaline pHs (pH > 9), the positive charge of adsorbent surface decrease and the adsorbent surface becomes negatively charged. There exit the ionic repulsion between the negatively charged surface and the anionic dye molecules, due to the abundance of OH^- and consequently the adsorption decreases. Also, at higher pH, there are no exchangeable anions on the outer surface of the adsorbent, thereby causing an adsorption decrease [12,16,37,38].

3.4. Adsorption isotherms

Several models are available to describe experimental data of adsorption isotherms. Three important isotherms, namely the Freundlich, Langmuir and Dubinin–Radushkevich isotherms, are the most frequently employed models. In this work, the data obtained from the adsorption experiments using RB K-GL at concentrations between 0 and 100 mg/l, the temperatures of 23, 28 and 33 °C, and at the dye solution initial pH were described with all the three models.

The Freundlich isotherm, which is an empirical equation employed to describe heterogeneous systems, was found to describe the equilibrium data well [39]. The equation for the linear fitting is

$$\ln\ Q_e = \ln\ K_F + \frac{1}{n}\ \ln\ C_e \tag{3}$$

where C_e and Q_e are the adsorbate equilibrium concentrations in the liquid (mg/l) and solid phases (mg/g), K_F (mg/g)(l/mg)$^{1/n}$ and n is the Freundlich constant related to adsorption capacity and adsorption intensity of the adsorbent, respectively. The values of K_F and n can be obtained from the intercept and slope, respectively, of the linear plot of experimental data of $\ln Q_e$

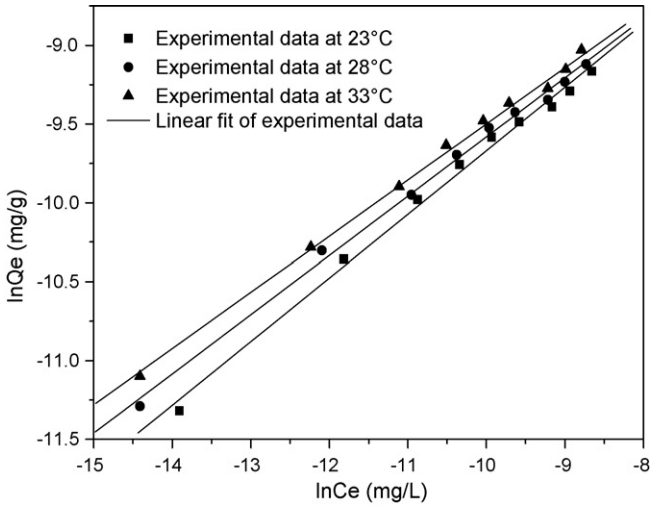

Fig. 5. The Freundlich isotherms for RB K-GL adsorption onto EPI-DMA/bentonite.

versus $\ln C_e$. Fig. 5 shows the Freundlich linear plots for the temperatures of 23, 28 and 33 °C.

The linear form of the Langmuir isotherm equation [40] is represented by

$$\frac{1}{Q_e} = \frac{1}{Q^0} + \left(\frac{1}{Q^0 K_L}\right)\frac{1}{C_e} \quad (4)$$

where Q^0 is the maximum adsorption capacity according to Langmuir monolayer adsorption (mg/g), and K_L is the constant according to the Langmuir model (l/mg). The plots of $1/Q_e$ versus $1/C_e$ for the adsorption of RB K-GL onto EPI-DMA/bentonite at various temperatures (Fig. 6) give straight lines with a slope of $1/Q^0K_L$ and an intercept of $1/Q^0$.

To distinguish the mechanisms involved in RB K-GL dye uptake by EPI-DMA/bentonite, the Dubinin–Radushkevitch (D–R) isotherm model was applied, which does not require an assumption of a homogeneous surface or constant adsorption potential [11]. It is based on the Polanyi theory [41,42]. Its widely used linear form is expressed as

$$\ln\ Q_e = \ln\ Q_m - \beta\varepsilon^2 \quad (5)$$

where Q_m is the theoretical saturation capacity (mg/g), β the constant related to the adsorption energy (mol^2/kJ^2), and ε is the Polanyi potential, which is equal to $-RT\ln(1 + 1/C_e)$. The plot of $\ln Q_e$ versus ε^2 gives β and Q_m from the slope and intercept, respectively. The D–R isotherm for RB K-GL adsorption onto EPI-DMA/bentonite at three different temperatures are shown in Fig. 7.

The parameters correlating with Langmuir, Freundlich and D–R models for the adsorption of RB K-GL onto EPI-DMA/bentonite are listed in Table 1. Applicability of the isotherm equations was always compared by judging the correlation coefficients, r^2 [16,41,43–47]. The equilibrium adsorption data obtained at the three temperatures are better represented by the Freundlich and D–R isotherm models with higher correlation coefficients in a range of 0.994–0.997 and 0.998–0.999, respectively, whereas the correlation coefficients for the Langmuir

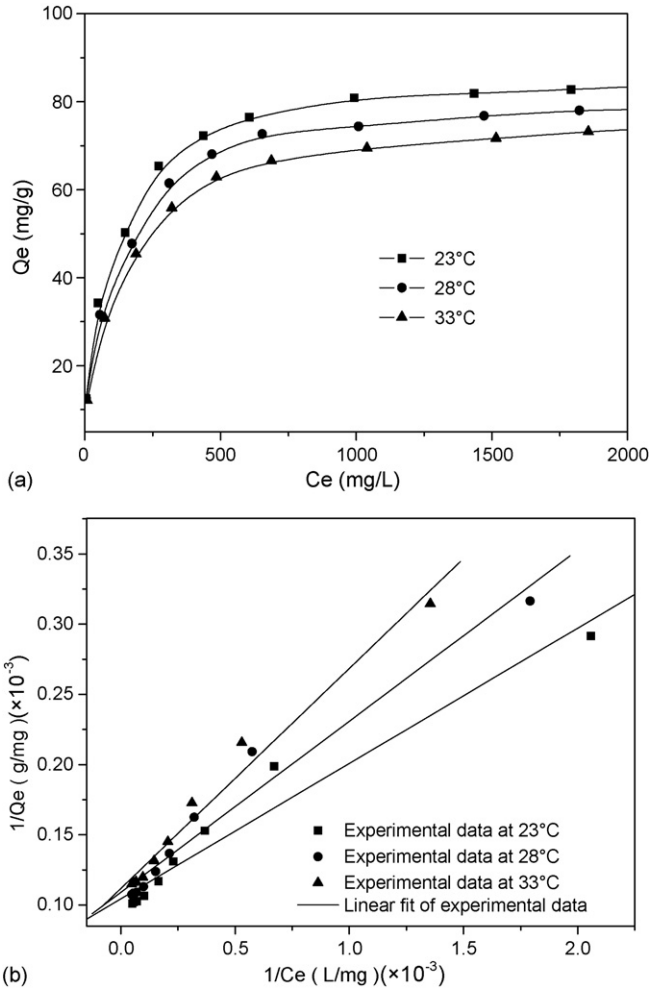

Fig. 6. The adsorption isotherms (a) and Langmuir isotherms (b) for RB K-GL adsorption onto EPI-DMA/bentonite.

isotherm model are between 0.940 and 0.974. It indicates that the surface of EPI-DMA/bentonite is mainly made up of heterogeneous adsorption patches [39] in addition to less homogeneous patches [11].

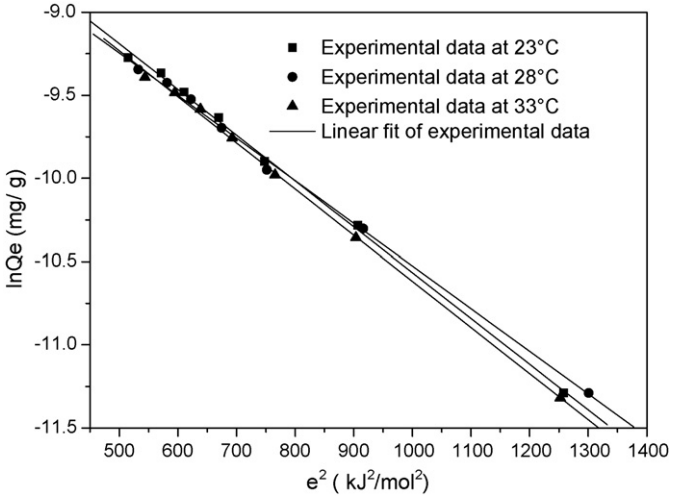

Fig. 7. The D-R isotherms for RB K-GL adsorption onto EPI-DMA/bentonite.

Table 1
Parameters obtained from Freundlich, Langmuir and D–R models

T (°C)	Freundlich			
	$1/n$	K_F ($\times 10^3$ (mg/g) (l/mg)$^{1/n}$)	r_F^2	ΔS.E. (%)
23	0.36	3.58	0.994	4.6
28	0.38	2.96	0.996	4.5
33	0.40	2.64	0.997	3.5

T (°C)	Langmuir			
	Q^0 (mg/g)	K_L (l/mg)	r_L^2	ΔS.E. (%)
23	68.60	100.53	0.954	4.7
28	65.69	147.73	0.940	4.9
33	64.46	158.64	0.974	4.5

T (°C)	Dubinin–Radushkevich				
	Q_m (mg/g)	β ($\times 10^3$ mol^2/kJ^2)	E (kJ/mol)	r_{D-R}^2	ΔS.E. (%)
23	309.67	2.75	13.48	0.998	3.4
28	299.70	2.64	13.76	0.999	3.2
33	266.74	2.48	13.98	*0.998*	3.4

Freundlich constant, n, is a measure of adsorption intensity. If the value of $1/n$ is below 1, reflecting favorable adsorption, then the adsorption capacity of adsorbent is large. As the value of $1/n$ increases, the adsorption bond becomes weak. As a result, when $1/n$ is above 1, unfavorable adsorption takes place [48]. As seen from Table 1, all the values of $1/n$ for EPI-DMA/bentonite are below 1 at the experimental temperatures, which is indicative of high adsorption intensity. But the increase of the values of $1/n$ along with the temperature increasing presents the decreasing trend of the adsorption capacity. The Freundlich constant, K_F, which are related to the adsorption capacity, also shows the trends.

From the D–R model, the adsorption mean free energy [$E = (-2\beta)^{-1/2}$], which is the energy required to transfer one mole of the adsorbate from solution to the surface of solid, was determined to evaluate the nature of interaction between the dye and the binding sites. As seen in Table 1, the values of E of RB K-GL dye adsorption onto EPI-DMA/bentonite at 23, 28 and 33 °C are 13.48, 13.76 and 13.98 kJ/mol, respectively, suggesting that the adsorption proceeded by ion exchange (E = 8–16 kJ/mol) [49] and the adsorption process can be explained as follows:

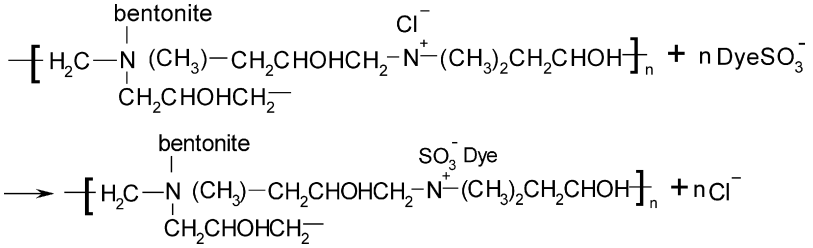

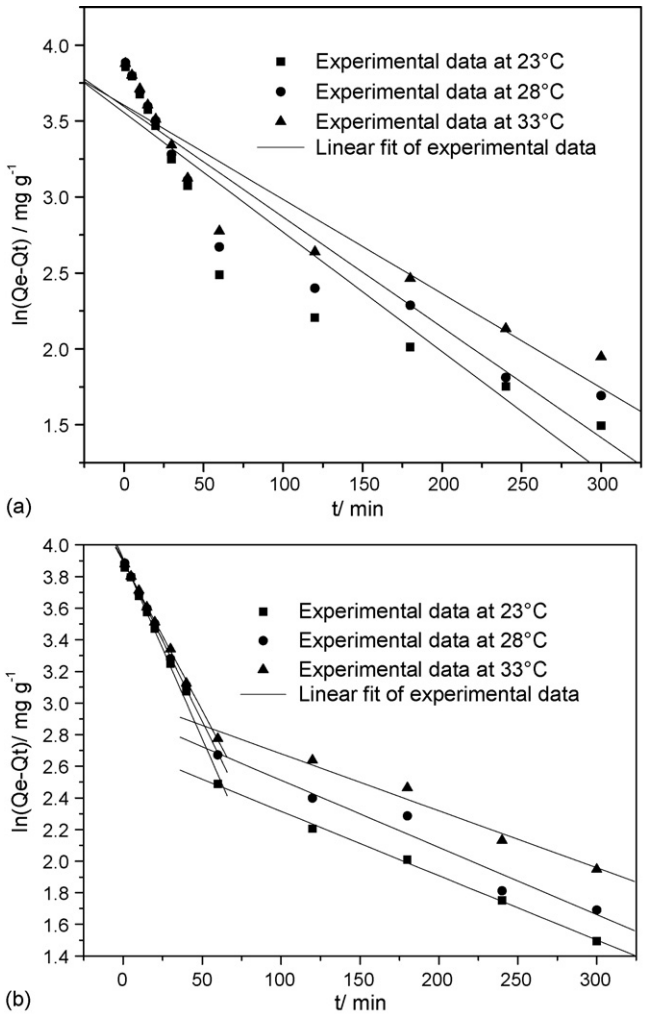

Fig. 8. Pseudo-first-order kinetic plots for RB K-GL adsorption onto EPI-DMA/bentonite ((a) whole adsorption process and (b) two steps adsorption process).

chemical reaction, experimental data related to the adsorption of RB K-GL onto EPI-DMA/bentonite at different temperatures were applied to several kinetic models including the pseudo-first-order equation, the pseudo-second-order equation and the intraparticle diffusion equation.

The pseudo-first-order kinetic model may be described by a differential equation

3.5. Adsorption kinetics

In order to investigate the controlling mechanism of the adsorption process, such as mass transfer, diffusion control and

$$\frac{dQ_1}{dt} = k_1(Q_1 - Q_t) \quad (6)$$

Table 2
Kinetic parameters for the adsorption of RB K-GL onto EPI-DMA/bentonite

T (°C)	Q_e (mg/g)	Pseudo-first-order model							
		Q_1 (mg/g)	k_1 ($\times 10^3$ min^{-1})	r_1^2	k_{1a} ($\times 10^3$ min^{-1})	r_{1a}^2	k_{1b} ($\times 10^3$ min^{-1})	r_{1b}^2	ΔS.E. (%)
23	47.70	36.79	7.87	0.887	22.75	0.993	4.25	0.998	3.1
28	46.32	36.47	7.26	0.902	20.33	0.999	4.07	0.962	3.8
33	44.49	35.05	6.21	0.893	18.79	0.999	3.60	0.978	3.3

T (°C)	Q_e (mg/g)	Pseudo-second-order model			
		k_2 ($\times 10^4$g/(mg min))	Q_2 (mg/g)	h (mg/min g)	r_2^2	ΔS.E. (%)
23	47.70	5.26	52.33	1.43	0.997	3.0
28	46.32	5.60	50.18	1.34	0.997	3.0
33	44.49	5.93	47.92	1.29	0.996	3.1

T (°C)	Intraparticle diffusion model				
	$k_{int,1}$ (mg/g min$^{1/2}$)	$r_{int,1}^2$	$k_{int,2}$ (mg/g min$^{1/2}$)	$r_{int,2}^2$	ΔS.E. (%)
23	5.39	0.985	0.78	0.997	3.0
28	5.23	0.992	0.96	0.985	4.7
33	5.00	0.990	0.98	0.987	4.3

The linear form of the equation after integration and rearrangement is

$$\ln(Q_1 - Q_t) = \ln Q_1 - k_1 t \tag{7}$$

where k_1 is the equilibrium rate constant of pseudo-first-order adsorption (min^{-1}), Q_1 and Q_t are the amounts of dyes adsorbed at equilibrium and at time t (mg/g), respectively. The plot of $\ln(Q_1 - Q_t)$ versus t gives a straight line, from which k_1 and Q_1 can be determined using the slope and intercept (Fig. 8a). All the calculated values under different temperatures are given in Table 2. However, in many cases the first-order kinetic model could not describe the whole range of adsorption time well with only one adsorption rate constant [39,50]. The plots in Fig. 8b indicate that two steps with two different k_{1a} and k_{1b} are taking place. It is noted that the magnitude of k_{1b} in all cases is much smaller than k_{1a}. Biswas and Chattoraj [51] have studied the adsorption kinetics of surfactants at solid–liquid interfaces, which were found to possess two steps with two rate constants. In the case of our study about the kinetics of disperse dyes adsorption at cationic polymer/bentonite surface, it was also found the two adsorption steps [52]. Similarly, for the case of adsorption of RB K-GL on EPI-DMA/bentonite, it could be explained that after some initial progress of adsorption with time, the surface of bentonite becomes crowded with adsorbed molecules of dye attached to its active spots with random orientations. After a certain elapse of time, the crowded molecules tend to orient in regular fashion, which may result in the creation of more vacant spaces for further adsorption of dye from the bulk to the surface [51]. Thereby, the adsorption process with two steps occurs. But this second process is much slower than the first process.

The pseudo-second-order equation, which is also based on the adsorption capacity of the solid phase, describes the process over the whole period of adsorption. This can be explained by the adsorption mechanism, which involves valency forces through sharing or exchange of electrons between dye anions and adsorbent [47]. The pseudo-second-order adsorption can be obtained from the following analysis:

$$\frac{dQ_t}{dt} = k_2(Q_2 - Q_t)^2 \tag{8}$$

Integrating Eq. (8) and considering $Q_t = 0$ at $t = 0$, a linear form is obtained

$$\frac{t}{Q_t} = \frac{1}{k_2 Q_2^2} + \frac{t}{Q_2} \tag{9}$$

where k_2 is the equilibrium rate constant of pseudo-second-order adsorption (g/mg min) and Q_2 is the equilibrium adsorption amount (mg/g) for the pseudo-second-order adsorption. Values of Q_2 and k_2 are calculated from the slope and intercept of the plots of t/Q_t against t (Fig. 9) and shown in Table 2 for comparison with the pseudo-first-order kinetic parameters. The initial

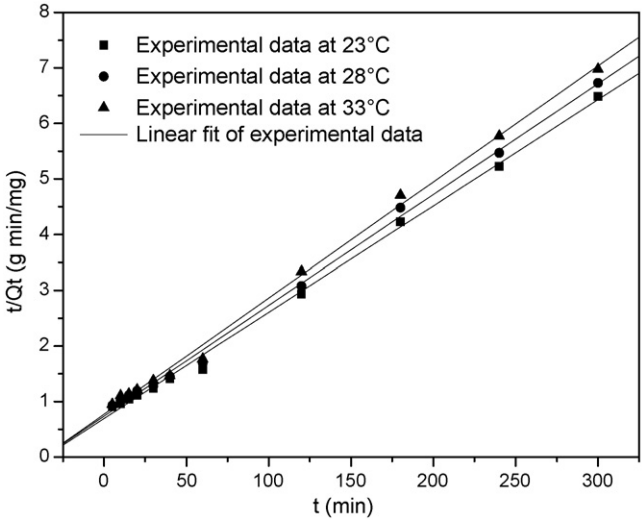

Fig. 9. Pseudo-second-order kinetic plots for RB K-GL adsorption onto EPI-DMA/bentonite.

adsorption rate h ($h = k_2 Q_2^2$) (mg/(g min)) [50,53] is also list in Table 2.

From the results in Table 2, the pseudo-second-order kinetic model could also describe the whole adsorption processes. In addition, the calculated Q_2 values for second-order also agree very well with the experimental Q_e values when comparing with the calculated Q_1 values for the first-order model.

The values of the calculated adsorption capacity of EPI-DMA/bentonite at equilibrium for RB K-GL, Q_2, drop from 52.33 to 47.92 mg/g, but the pseudo-second-order rate constants, k_2, show a steady increase from 5.26×10^{-4} to 5.93×10^{-4} g/(mg min) with the temperature increasing from 23 to 33 °C. These suggest that high temperature does not favor the increase of adsorption capacity but can accelerate the adsorption processing. The results also indicate that the mechanism associated with the adsorption of RB K-GL onto EPI-DMA/bentonite involves a physical process, according to Ho and McKay [54] who report that in conventional physisorption systems, increasing temperature usually decreases the equilibrium capacity, but increases the adsorption rate of approach to equilibrium.

Adsorption kinetics is usually controlled by different mechanisms. The pseudo-first-order and pseudo-second-order kinetic models cannot identify the diffusion mechanism. The possibility of intraparticle diffusion is examined by using the intraparticle diffusion model:

$$Q_t = k_{\text{int}} t^{0.5} + C \tag{10}$$

where k_{int} is the intraparticle diffusion rate constant (mg/(g min$^{1/2}$)), Q_t the amount of dye adsorbed at time t (mg/g) and C is the constant, which is proportional to the boundary layer thickness. Such process may include a first sharper portion (stage 1) attributed to boundary layer diffusion or the external diffusion; a surface adsorption stage (stage 2), which is a gradual adsorption stage due to intraparticle diffusion; and followed by a final equilibrium stage (stage 3) where intraparticle diffusion slows down due to the low concentrations in the solution [55–57].

The plot of Q_t versus $t^{0.5}$ would result in a linear relationship with a slope of k_{int} and an intercept of C when adsorption mechanism follows the intraparticle diffusion process. If this line passed through the origin, the particle diffusion would be the controlling step [58]. Otherwise, the intraparticle diffusion is not the only rate-controlling step but some degree of boundary layer diffusion also control the adsorption. Moreover, other adsorption kinetic processes may be operating simultaneously.

According to Özacar and Şengil [57], in the case of intraparticle diffusion model, the plots can present a multi-linearity (Fig. 10b), indicating that two steps with two different $k_{\text{int},1}$ and $k_{\text{int},2}$ are taking place. Based on the former discussion about the pseudo-first-order kinetic model, it can be found that all the plots indicate the same general features, initial linear portion (stage 2, 1–60 min) where both intraparticle diffusion and first-order kinetics reaction occur [59], followed by a plateau (stage 3, after 60 min), where the intra-particle diffusion and first-order reaction slow down. In addition, the calculated values of intraparticle

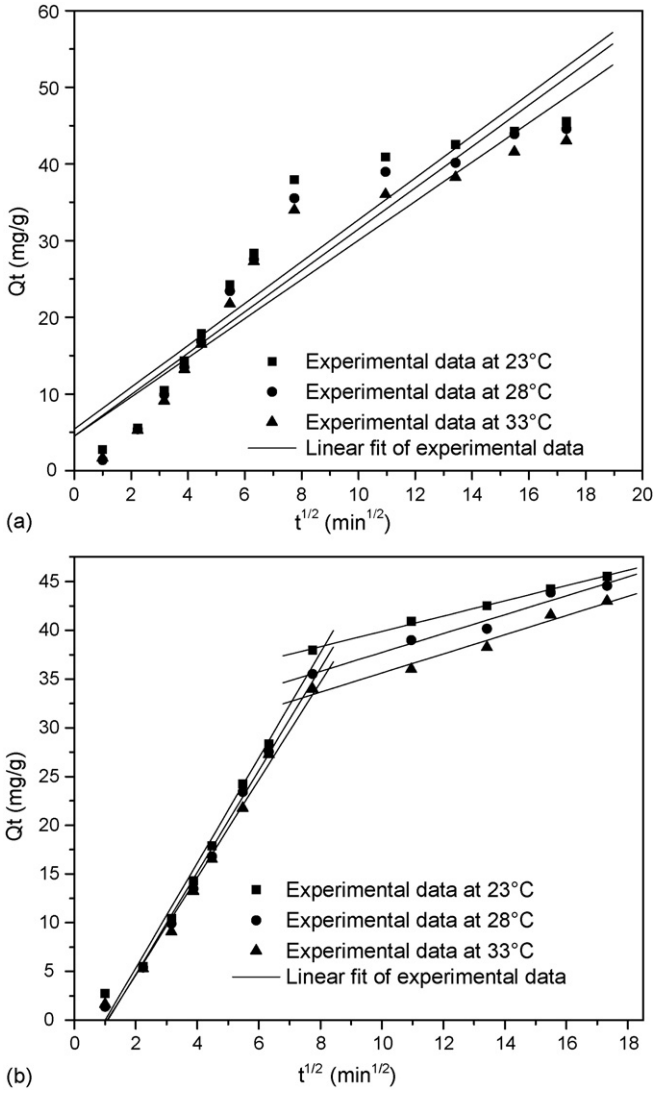

Fig. 10. Intraparticle diffusion plots for RB K-GL adsorption onto EPI-DMA/bentonite ((a) whole adsorption process and (b) two steps adsorption process).

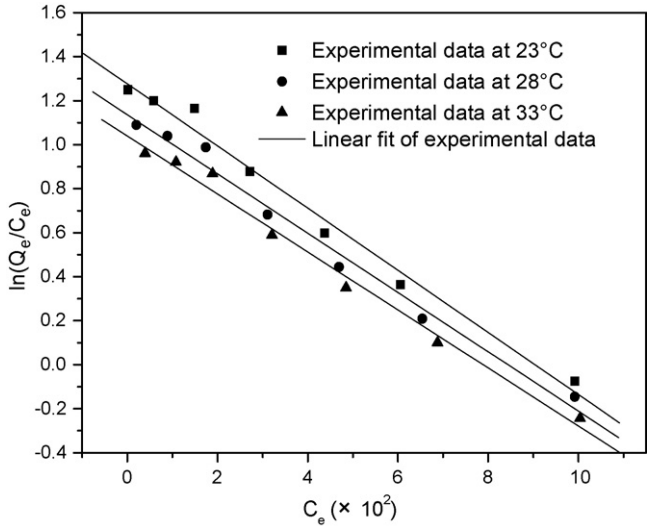

Fig. 11. Plots of $\ln(Q_e/C_e)$ vs. C_e at different temperatures.

Table 3
Thermodynamic parameters for adsorption of RB K-GL dye onto EPI-DMA/bentonite

T (°C)	K_s (kg^{-1})	ΔG°_{ads} (kJ/mol)	ΔH°_{ads} (kJ/mol)	ΔS°_{ads} (J/mol K)	ΔS.E. (%)
23	3583.82	−3.14			5.0
28	3117.06	−2.86	−17.91	−49.92	4.8
33	2818.74	−2.65			4.5

diffusion rate constants, $k_{int,1}$ and $k_{int,2}$ for two adsorption steps, which have better correlation coefficients (r^2_{int1} and r^2_{int1}) than k_{int} for the whole adsorption process does, also agree with the two steps adsorption. In addition, the first sharper portion (stage 1) as reported [55–57] is not described in the present study due to fast completion within 1 min. But the values of the intercept of the plots, C, indicate that some degree of boundary layer control may be operating simultaneously in the adsorption process.

3.6. Thermodynamic parameters

The dependence of thermodynamic equilibrium constant (K_s) on temperature can be used to estimate thermodynamic parameters, including the free energy changes (ΔG°_{ads}), standard enthalpy changes (ΔH°_{ads}) and the entropy changes (ΔS°_{ads}) associated with the adsorption process. It can be calculated by

$$\Delta G^\circ_{ads} = -RT \ln K_s \quad (11)$$

$$\ln K_s = -\frac{\Delta H^\circ_{ads}}{RT} + \frac{\Delta S^\circ_{ads}}{R} \quad (12)$$

The values of K_s are obtained by plotting $\ln Q_e/C_e$ versus C_e and extrapolating to $C_e = 0$ (Fig. 11) as suggested by Khan and Singh [60,61]. The plot of $\ln K_s$ against $1/T$ (Fig. 12) yields a straight line, from which the value of ΔH°_{ads} and ΔS°_{ads} can be calculated from the slope and intercept, respectively. The results are listed in Table 3.

The Gibbs free energy change ΔG°_{ads} is in the range of −3.14 to −2.65 kJ/mol, which indicates that the process is spontaneous. Moreover, based on the decrease in ΔG°_{ads} with increase in temperature, it indicates that the presence of an energy barrier at high temperature in adsorption. Therefore, adsorption is less favorable at high temperatures. This is also verified by the adsorption isotherm studies. The enthalpy change ΔH°_{ads} (−17.91 kJ/mol) of the system is negative and lower than 40 kJ/mol, indicating that the adsorption of RB K-GL dye onto EPI-DMA/bentonite is exothermic and physical in nature, involving weak forces of attraction [16,62]. In addition, the negative standard entropy change (ΔS°_{ads}) value (−49.92 J/mol K) implies that the regular degree of the adsorption system increases due to the freedom degree of the adsorbed species decrease.

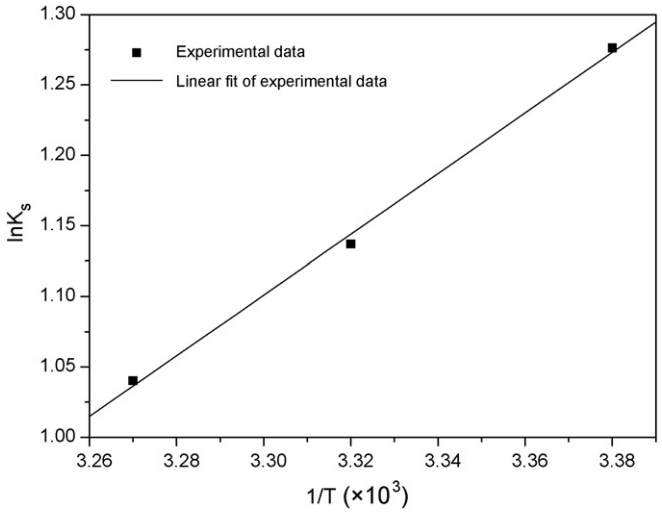

Fig. 12. Plot of $\ln K_s$ vs. $1/T$.

4. Conclusion

An alternative method of intercalation, employing ultrasonics, was adopted to prepare cationic polyelectrolyte/bentonite with EPI-DMA. Compared with raw bentonite, the basal spacing of EPI-DMA/bentonite expands from 12.54 to 16.91 Å and the hydrophobic nature is improved obviously.

The EPI-DMA/bentonite adsorption capacity for reactive dye RB K-GL was obviously effected by the pH value of the solution. The adsorption pattern of RB K-GL dye onto EPI-DMA/bentonite at 23, 28 and 33 °C was better described by the Freundlich and Dubinin–Radushkevich isotherms than by the Langmuir isotherms. The adsorption capacity of EPI-DMA/bentonite decreased with increasing temperature during the adsorption process of dye. The Freundlich constant n reflects that the EPI-DMA/bentonite is favorable adsorbent for RB K-GL dye. The mean energy of adsorption (E) calculated from the D–R isotherm indicates that the adsorption proceeded with ion exchange.

Pseudo-first- and second-order kinetic models and intraparticle diffusion kinetic models were developed to study the kinetics of the adsorption process. Both intraparticle diffusion and pseudo-first-order adsorption kinetic were involved up 60 min of adsorption process, whereas the pseudo-second-order kinetic model is suitable for the whole process.

Negative ΔG°_{ads} shows that the adsorption of RB K-GL dye onto EPI-DMA/bentonite is carried out spontaneously at the studied temperatures. Moreover, the decrease in ΔG°_{ads} with increase in temperature suggests that the adsorption is less favorable at high temperatures. The negative enthalpy change ΔH°_{ads} (−17.91 kJ/mol) of the system indicates that the adsorption process is exothermic and physical in nature, involving weak forces of attraction. In addition, the standard entropy change ΔS°_{ads} is negative, implying a decreased random at the solid/solution interface.

It is concluded that the ultrasonic synthesized EPI-DMA/bentonite is an effective adsorbent for removing RB K-GL dye from aqueous solution at room temperature. It is a suitable adsorbent, representing environmentally clean utilization of wastewater.

Acknowledgement

The authors are thankful to the support of the Shandong Provincial Foundation of Natural Sciences, China.

References

[1] X.Y. Yang, B. Al-Duri, Application of branched pore diffusion model in the adsorption of reactive dyes on activated carbon, Chem. Eng. J. 83 (2001) 15–23.
[2] T. O'Mahony, E. Guibal, J.M. Tobin, Reactive dye biosorption by Rhizopus arrhizus biomass, Enzyme Microb. Technol. 31 (2002) 456–463.
[3] S. Netpradit, P. Thiravetyan, S. Towprayoon, Evaluation of metal hydroxide sludge for reactive dye adsorption in a fixed-bed column system, Water Res. 38 (2004) 71–78.
[4] P.V. Messina, P.C. Schulz, Adsorption of reactive dyes on titania–silica mesoporous materials, J. Colloid Interf. Sci. 299 (2006) 305–320.
[5] A. Gülbahar, U. İlhan, G. Fuat, Kinetics of the adsorption of reactive dyes by chitin, Dyes Pigments 73 (2007) 168–177.
[6] S. Papic, N. Koprivanac, A.L. Bozic, A. Metes, Removal of some reactive dyes from synthetic wastewater by combined Al(III) coagulation/carbon adsorption process, Dyes Pigments 62 (2004) 291–298.
[7] N.H. Ince, G. Tezcanlí, Reactive dyestuff degradation by combined sonolysis and ozonation, Dyes Pigments 49 (2001) 145–153.
[8] G.M. Walker, L. Hansen, J.A. Hana, S.J. Allen, Kinetics of a reactive dye adsorption onto dolomitic sorbents, Water Res. 37 (2003) 2081–2089.
[9] C. Namasivayam, R. Radhika, S. Suba, Uptake of dyes by a promising locally available agricultural solid waste: coir pith, Waste Manage. 21 (2001) 381–387.
[10] Y.S. Ho, G. McKay, A kinetic study of dye sorption by biosorbent waste product pith, Resour. Conserv. Recycle 25 (1999) 171–193.
[11] A.S. Özcan, B. Erdem, A. Özcan, Adsorption of Acid Blue 193 from aqueous solutions onto BTMA-bentonite, Colloid Surface. A: Physicochem. Eng. Aspects. 266 (2005) 73–81.
[12] M. Özacar, İ.A. Şengil, Adsorption of reactive dyes on calcined alunite from aqueous solutions, J. Hazard. Mater. 98 (2003) 211–224.
[13] M. Doğan, M. Alkan, Adsorption kinetics of methyl violet onto perlite, Chemosphere 50 (2003) 517–528.
[14] S.Y. Lee, S.J. Kim, Adsorption of naphthalene by HDTMA modified kaolinite and halloysite, Appl. Clay Sci. 22 (2002) 55–63.
[15] S.M. Koh, J.B. Dixon, Preparation and application of organominerals as sorbents of phenol, benzene and toluene, Appl. Clay Sci. 18 (2001) 111–122.
[16] A.S. Özcan, B. Erdem, A. Özcan, Adsorption of Acid Blue 193 from aqueous solutions onto Na-bentonite and DTMA-bentonite, J. Colloid Interf. Sci. 280 (2004) 44–54.
[17] M. Akçay, Characterization and determination of the thermodynamic and kinetic properties of *p*-CP adsorption onto organophilic bentonite from aqueous solution, J. Colloid Interf. Sci. 280 (2004) 299–304.
[18] Y.H. Shen, Preparations of organobentonite using nonionic surfactants, Chemosphere 44 (2001) 989–995.
[19] G.J. Churchman, Formation of complexes between bentonite and different cationic polyelectrolytes and their use as sorbents for non-ionic and anionic pollutants, Appl. Clay Sci. 21 (2002) 177–189.
[20] M. Borah, J.N. Ganguli, D.K. Dutta, Intersalation reactions of trisdiimine metal complexes with montmorillonite clay: a new approach, J. Colloid Interf. Sci. 233 (2001) 171–179.
[21] J.Zh. Wang, Y. Hu, Sh.F. Wang, Z.Y. Chen, Sonochemical one-directional growth of montmorillonite–polystyrene nanocomposite, Ultrason. Sonochem. 12 (2005) 165–168.
[22] J.Z. Wang, Y. Hu, Y. Tang, Z.Y. Chen, Preparation of nanocomposite of polyaniline and gamma-zirconium phosphate (γ-ZrP) by power ultrasonic irradiation, Mater. Res. Bull. 38 (2003) 1301–1308.
[23] C. Breen, R. Watson, Polycation-exchanged clays as sorbents for organic pollutants. Influence of layer charge on sorption capacity, J. Colloid Interf. Sci. 208 (1998) 422–429.
[24] G. Durand-Piana, F. LaFuma, R. Audebert, Flocculation and adsorption properties of cationic polyelectrolytes toward Na-montmorillonite dilute suspensions, J. Colloid Interf. Sci. 119 (1987) 474–480.
[25] C. Breen, J.O. Rawson, B.E. Mann, Adsorption of polycations on clays: an in situ study using 133Cs solution-phase NMR, J. Mater. Chem. 6 (1996) 253–260.
[26] X.P. Ma, X.Q. Fu, D.B. Zhao, W.X. Wan, H. Yuan, Synthesis of epicholorothydrin-dimethylamine cationic polymer, Polym. Mater. Sci. Eng. 12 (1996) 50–53 (in Chinese).
[27] Q. Li, Q.Y. Yue, B.Y. Gao, L.L. Liu, Properties of and decoloration of orcein dye on epicholorohydrin-dimethylamine cationic polymer/bentonite nanocomposite adsorption material, J. Chem. Ind. Eng. (China) 57 (2006) 436–441.
[28] Q. Li, Q.Y. Yue, B.Y. Gao, L.L. Liu, Kinetics of adsorption of disperse dyes at cationic bentonite, Chem. J. Chin. Univ. 27 (2006) 1113–1117.
[29] R.K. Taylor, Cation exchange in clays and mudrocks by methylene blue, J. Chem. Technol. Biotech. A 35 (1985) 195–207.
[30] T.A. Wolfe, T. Demirel, E.R. Baumann, Interaction of aliphatic amines with montmorillonite to enhance adsorption of organic pollutants, Clay Clay Miner. 33 (1985) 301–311.
[31] C. Breen, The characterisation and use of polycation-exchanged bentonites, Appl. Clay Sci. 15 (1999) 187–219.
[32] Q.-Y. Yue, Q. Li, B.-Y. Gao, A.-J. Yuan, Y. Wang, Formation and characteristics of cationic-polymer/bentonite complexes as adsorbents for dyes, Appl. Clay Sci. 35 (2007) 268–275.
[33] Y. Yu, Y. Li, Y.Y. Zhuang, B.P. Xin, Q.M. Zou, Preliminary study of the relationship between the structure of dyes flocculated by PAN- DCD and the decolorization efficiency of dyes, Urban Environ. Urban Ecol. 1 (2000) 16–19 (in Chinese).
[34] A. Özcan, Ç. Ömeroğlu, Y. Erdoğan, A.S. Özcan, Modification of bentonite with a cationic surfactant: an adsorption study of textile dye Reactive Blue 19, J. Hazard. Mater. 140 (2007) 173–179.
[35] J.J.M. Órfão, A.I.M. Silva, J.C.V. Pereira, S.A. Barata, I.M. Fonseca, P.C.C. Faria, M.F.R. Pereira, Adsorption of a reactive dye on chemically modified activated carbons—influence of pH, J. Colloid Interf. Sci. 296 (2006) 480–489.
[36] A.S. Özcan, A. Özcan, Adsorption of acid dyes from aqueous solutions onto acid-activated bentonite, J. Colloid Interf. Sci. 276 (2004) 39–46.
[37] Z. Wu, I.-S. Ahn, C.-H. Lee, J.-H. Kim, Y.G. Shul, K. Lee, Enhancing the organic dye adsorption on porous xerogels, Colloids Surf. A: Physicochem. Eng. Aspect 240 (1–3) (2004) 157–164.
[38] C. Namasivayam, R.T. Yamuna, D. Arasi, Removal of procion orange from wastewater by adsorption on waste red mud, Sep. Sci. Technol. 37 (10) (2002) 2421–2431.
[39] Z. Aksu, D. Dönmez, A comparative study on the biosorption characteristics of some yeasts for Remazol Blue reactive dye, Chemosphere 50 (2003) 1075–1083.
[40] C. Namasivayam, R.T. Yamuna, Waste biogas residual slurry for the removal of Pb(II) from aqueous solution and radiator manufacturing industry wastewater, Bioresour. Technol. 5 (1995) 125–131.
[41] M. Akçay, G. Akçay, The removal of phenolic compounds from aqueous solutions by organophilic bentonite, J. Hazard. Mater. B 113 (2004) 189–193.
[42] S.H. Lin, R.S. Juang, Heavy metal removal from water by sorption using surfactant-modified montmorillonite, J. Hazard. Mater. 92 (2002) 315–326.
[43] M.J. Iqbal, M.N. Ashiq, Adsorption of dyes from aqueous solutions on activated charcoal, J. Hazard. Mater. B 139 (2007) 57–66.

[44] Y. Aşçı, M. Nurbaş, Y.S. Açıkel, Sorption of Cd(II) onto kaolin as a soil component and desorption of Cd(II) from kaolin using rhamnolipid biosurfactant, J. Hazard. Mater. B 139 (2007) 50–56.
[45] M.S. Onyango, Y. Kojima, O. Aoyi, E.C. Bernardo, Adsorption equilibrium modeling and solution chemistry dependence of fluoride removal from water by trivalent-cation-exchanged zeolite F-9, J. Colloid Interf. Sci. 279 (2004) 341–350.
[46] W.T. Tsai, C.Y. Chang, C.H. Ing, C.F. Chang, Adsorption of acid dyes from aqueous solution on activated bleaching earth, J. Colloid Interf. Sci. 275 (2004) 72–78.
[47] Z. Eren, F.N. Acar, Adsorption of Reactive Black 5 from an aqueous solution: equilibrium and kinetic studies, Desalination 194 (2006) 1–10.
[48] W.T. Tsai, C.W. Lai, K.J. Hsien, Effect of particle size of activated clay on the adsorption of paraquat from aqueous solution, J. Colloid Interf. Sci. 263 (2003) 29–34.
[49] M. Mahramanlioglu, I. Kizilcikli, I.O. Bicer, Adsorption of fluoride from aqueous solution by acid treated spent bleaching earth, J. Fluorine Chem. 115 (2002) 41–47.
[50] M. Özacar, I.A. Şengil, Adsorption of reactive dyes on calcined alunite from aqueous solutions, J. Hazard. Mater. 40 (2003) 1–14.
[51] S.C. Biswas, D.K. Chattoraj, Kinetics of adsorption of cationic surfactants at silica–water interface, Colloid Interf. Sci. 205 (1998) 12–20.
[52] Q.-Y. Yue, Q. Li, B.-Y. Gao, Y. Wang, Kinetics of adsorption of disperse dyes by polyepicholorohydrin-dimethylamine cationic polymer/bentonite, Sep. Purif. Technol. 54 (2007) 279–290.
[53] Y.S. Ho, G. McKay, Pseudo-second-order model for sorption processes, Process Biochem. 34 (1999) 451–465.
[54] Y.S. Ho, G. McKay, Sorption of dye from aqueous solution by peat, Chem. Eng. J. 70 (1998) 115–124.
[55] A. Özcan, E.M. Öncü, A.S. Özcan, Adsorption of Acid Blue 193 from aqueous solutions onto DEDMA-sepiolite, J. Hazard. Mater. B 129 (2006) 244–252.
[56] E. Guibal, P. McCarrick, J.M. Tobin, Comparison of the sorption of anionic dyes on activated carbon and chitosan derivatives from dilute solutions, Sep. Sci. Technol. 38 (2003) 3049–3073.
[57] M. Özacar, İ.A. Şengil, Application of kinetic models to the sorption of disperse dyes onto alunite, Colloids Surf. A: Physicochem. Eng. Aspects 242 (2004) 105–113.
[58] J.P. Chen, S. Wu, K.-H. Chong, Surface modification of a granular activated carbon by citric acid for enhancement of copper adsorption, Carbon 41 (2003) 1979–1986.
[59] H.L. Frisch, Diffusion with first-order reaction with a time-dependent rate coefficient, J. Colloid Interf. Sci. 153 (1992) 292–293.
[60] A.A. Khan, R.P. Singh, Adsorption thermodynamics of carbofuran on Sn(IV) arsenosilicate in H^+, Na^+ and Ca^{2+} forms, Colloid Surf. 24 (1987) 33–42.
[61] A. Demirbas, A. Sari, O. Isildak, Adsorption thermodynamics of stearic acid onto bentonite, J. Hazard. Mater. B 135 (2006) 226–231.
[62] B. von Oepen, W. Kördel, W. Klein, Sorption of nonpolar and polar compounds to soils: processes, measurements and experience with the applicability of the modified OECD-Guideline 106, Chemosphere 22 (1991) 285–304.